



UvA-DARE (Digital Academic Repository)

Swallow Tail Sign

Revisited

Brammerloh, M.; Kirilina, E.; Alkemade, A.; Bazin, P.-L.; Jantzen, C.; Jäger, C.; Herrler, A.; Pine, K.J.; Gowland, P.A.; Morawski, M.; Forstmann, B.U.; Weiskopf, N.

DOI

[10.1148/radiol.212696](https://doi.org/10.1148/radiol.212696)

Publication date

2022

Document Version

Final published version

Published in

Radiology

License

CC BY

[Link to publication](#)

Citation for published version (APA):

Brammerloh, M., Kirilina, E., Alkemade, A., Bazin, P.-L., Jantzen, C., Jäger, C., Herrler, A., Pine, K. J., Gowland, P. A., Morawski, M., Forstmann, B. U., & Weiskopf, N. (2022). Swallow Tail Sign: Revisited. *Radiology*, *305*(3), 674–677. <https://doi.org/10.1148/radiol.212696>

General rights

It is not permitted to download or to forward/distribute the text or part of it without the consent of the author(s) and/or copyright holder(s), other than for strictly personal, individual use, unless the work is under an open content license (like Creative Commons).

Disclaimer/Complaints regulations

If you believe that digital publication of certain material infringes any of your rights or (privacy) interests, please let the Library know, stating your reasons. In case of a legitimate complaint, the Library will make the material inaccessible and/or remove it from the website. Please Ask the Library: <https://uba.uva.nl/en/contact>, or a letter to: Library of the University of Amsterdam, Secretariat, P.O. Box 19185, 1000 GD Amsterdam, The Netherlands. You will be contacted as soon as possible.

Swallow Tail Sign: Revisited

Malte Brammerloh, MSc • Evgeniya Kirilina, PhD • Anneke Alkemade, PhD • Pierre-Louis Bazin, PhD • Caroline Jantzen, BSc • Carsten Jäger, PhD • Andreas Herrler, PhD • Kerrin J. Pine, PhD • Penny A. Gowland, PhD • Markus Morawski, MD, PhD • Birte U. Forstmann, PhD • Nikolaus Weiskopf, PhD

From the Department of Neurophysics, Max Planck Institute for Human Cognitive and Brain Sciences, Stephanstr 1a, 04103 Leipzig, Germany (M.B., E.K., P.L.B., C. Jantzen, C. Jäger, K.J.P., M.M., N.W.); International Max Planck Research School on Neuroscience of Communication: Function, Structure, and Plasticity, Leipzig, Germany (M.B.); Felix Bloch Institute for Solid State Physics, Faculty of Physics and Earth Sciences, Leipzig University, Leipzig, Germany (M.B., N.W.); Center for Cognitive Neuroscience Berlin, Free University Berlin, Berlin, Germany (E.K.); Integrative Model-based Cognitive Neuroscience Research Unit, University of Amsterdam, Amsterdam, the Netherlands (A.A., P.L.B., B.U.F.); Department of Anatomy and Embryology, Maastricht University, Maastricht, the Netherlands (A.H.); Sir Peter Mansfield Imaging Centre, School of Physics & Astronomy, University of Nottingham, Nottingham, UK (P.A.G.); and Paul Flechsig Institute–Center of Neuropathology and Brain Research, Faculty of Medicine, Universität Leipzig, Leipzig, Germany. Received October 28, 2021; revision requested December 22; final revision received May 2, 2022; accepted June 6. **Address correspondence to** M.B. (email: mbrammerloh@cbs.mpg.de).

The research leading to these results has received funding from the European Research Council under the European Union's Seventh Framework Programme (FP7/2007-2013)/European Research Council grant agreement no. 616905. N.W. has received funding from the BMBF (01EW1711B) in the framework of ERA-NET NEURON. This research was financially supported by STW/NWO, NWO VICI, the Brain Foundation of the Netherlands, and Stichting Internationaal Parkinson Fonds. M.B. has received funding from the International Max Planck Research School on Neuroscience of Communication: Function, Structure, and Plasticity. N.W. has received funding from the European Union's Horizon 2020 research and innovation programme under the grant agreement no. 681094. Aspects of this work were supported by funding from the Deutsche Forschungsgemeinschaft Priority Program 2041 "Computational Connectomics," MO 2249/3-1 and MO 2249/3-2 and the Alzheimer Forschungsinitiative e.V. (AFI #18072) to M.M. A.A. is financially supported by JPND/ZonMW (grant 73305113). A.A.'s work is financially supported by JPND/ZonMW (grant 73305113); N.W.'s work is financially supported by JPND/Federal Ministry of Education and Research under support code 01ED2210.

Conflicts of interest are listed at the end of this article.

Radiology 2022; 305:674–677 • <https://doi.org/10.1148/radiol.212696> • Content codes:   • Published under a CC BY 4.0 license

The loss of the radiologic swallow tail sign on MRI scans of the substantia nigra is a promising diagnostic marker of Parkinson disease (1), although its anatomic underpinning is unclear. An early influential study showed that the hyperintense inner part of the swallow tail sign on T2*-weighted images (STh) corresponds to iron-poor areas in substantia nigra and suggested it to equal nigrosome 1, the dopaminergic region affected earliest and strongest in Parkinson disease (2). This would render the STh a cellularly specific marker (2). However, recent postmortem tissue studies have challenged this interpretation, reporting that nigrosome 1 is hypointense in T2*-weighted images (3,4). We combined three-dimensional histology with 7-T in vivo and postmortem MRI to demonstrate that nigrosome 1 and the radiologic STh are partially overlapping but distinct.

Materials and Methods

In this secondary analysis of prospectively collected data, 7-T in vivo MRI (5) was combined with 7-T postmortem MRI, three-dimensional block-face imaging, and immunohistochemistry (6). The local ethics committees approved all studies.

From March to December 2017, in vivo T2*-weighted images with 0.4-mm isotropic resolution were acquired in three randomly chosen healthy volunteers with no contraindication to ultra-high-field MRI investigation to match the number of postmortem specimens (Fig 1) (5).

Postmortem T2*-weighted images were acquired, using a similar protocol and the same resolution as for in vivo images, of three whole heads (specimens 1, 7, and 8 in a previous study [6]) and complemented by high-quality histochemistry in the substantia nigra (Fig 2). Brain specimens from donors with no record of neurologic disease were sourced through a whole-body donation program. Written informed consent for whole-body donation had been provided before death.

To assess intrarater reliability, one author (P.A.G., with 9 years of experience in MRI in Parkinson disease) delineated the STh twice on in vivo T2*-weighted images (Figs 1B, 2B).

A neuroanatomist (M.M., with 20 years of experience) and a trained research assistant (C. Jantzen, with 1 year of experience) segmented areas with a high density of neuromelanin-pigmented dopaminergic neurons on block-face images (resolution, 150 × 150 × 200 μm³) while blinded to the STh delineation. Nigrosome 1 was defined as a subvolume with the characteristic "stripe" morphology (2) (Fig 1D, 1E). It agreed with the classic definition of nigrosome 1 based on low anticalbindin immunoreactivity (not shown here).

In vivo and postmortem T2*-weighted MRI scans and block-face images were affinely registered based on anatomic landmarks, including small vessels, outside the substantia nigra. Before comparing STh and nigrosome 1, segmentations were smoothed with a kernel reflecting the registration error (0.46 mm, Fig 1). One author (M.B., with 5 years of experience) assessed size differences using the Student *t* test. Two-tailed *P* < .05 was indicative of a statistically significant difference.

Results

Three female participants (mean age, 30 years ± 1 [SD]) and three postmortem brains (mean age, 78 years ± 3; two male donors) were evaluated.

Although the STh was ovoid-shaped for all participants, nigrosome 1 was consistently flat and disk-like (Fig 1E). Nigrosome 1 was significantly thinner (*P* < .001) and longer (*P* = .003) than the STh (Fig 2F).

Coregistration of in vivo and postmortem T2*-weighted MRI scans to block-face images showed that nigrosome 1 only partly overlapped with STh for all possible combinations of data sets across participants and specimens. Nigrosome 1 extended beyond the STh

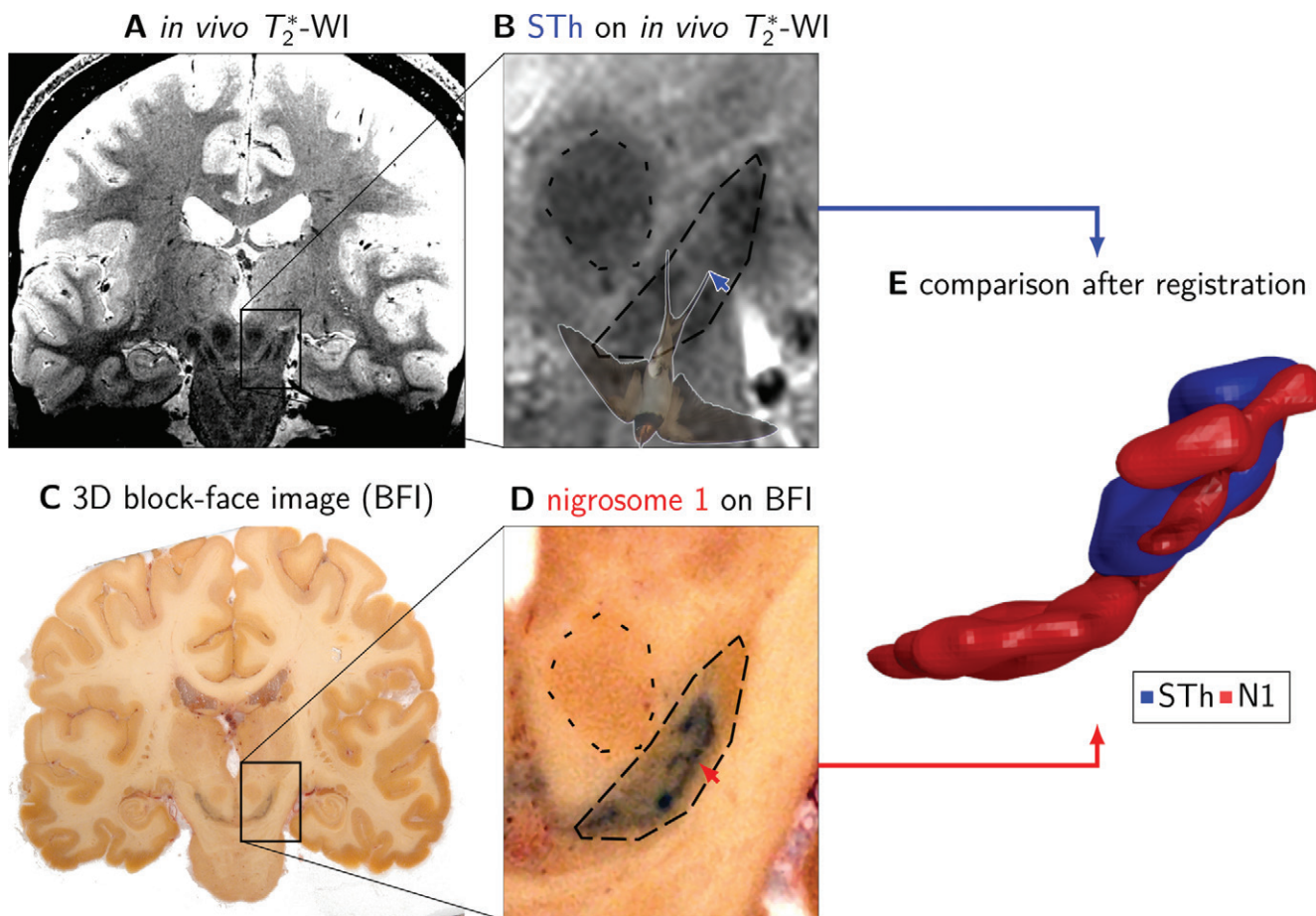


Figure 1: Spatial relationship of the hyperintense inner part of the swallow tail sign on T_2^* -weighted images (STh) and nigrosome 1 (N1) revealed by a combination of in vivo MRI and postmortem three-dimensional (3D) histochemistry. **(A, B)** In vivo T_2^* -weighted images (T_2^* -WI) in a 29-year-old woman. The STh (arrow in **B**) was segmented as a hyperintense patch in the substantia nigra and is surrounded by larger hypointense structures that resemble the tail of a swallow (see swallow overlay in **B**). The boundary of the substantia nigra is indicated with long dashes, and the red nucleus is indicated with short dashes (**B**). **(C, D)** Postmortem 3D block-face images (BFI) obtained during histochemistry examination in a 75-year-old female donor. The dopaminergic region nigrosome 1 was segmented as a dark-pigmented stripe (arrow in **D**). The boundary of the substantia nigra is indicated with long dashes, and the red nucleus is indicated with short dashes. A low calbindin immunoreactivity in one specimen corroborated the nigrosome 1 segmentation (not shown). **(E)** An affine, landmark-based coregistration of in vivo and postmortem data enabled the comparison of the radiologic STh and histologically defined nigrosome 1. The registration accuracy was $0.193 \text{ mm} \pm 0.012$ (mean \pm SD) between block-face and postmortem T_2^* -weighted images and $0.46 \text{ mm} \pm 0.06$ (mean \pm SD across data set combinations) between block-face and in vivo images.

in anteroposterior and superoinferior directions (Fig 2F). On postmortem MRI scans and block-face images, nigrosome 1 consistently appeared as a thin, dark stripe (Fig 2C, 2E).

Discussion

We showed that the widespread equation of the STh and nigrosome 1 is inaccurate because they are only partially overlapping. Therefore, STh and nigrosome 1 probably correspond to distinct structures and should not be used synonymously.

The hypointense appearance of nigrosome 1 on postmortem T_2^* -weighted images, unlike the hyperintense STh, is consistent with findings of postmortem tissue studies (3,4). It is unclear why nigrosome 1 has not been reported as a hypointense structure on in vivo scans, but causes may include an insufficient contrast-to-noise ratio, image artifacts, or different contrast mechanisms in nigrosome 1 between in vivo and postmortem imaging.

Our study had limitations, including the small number of histologic samples and the age and sex differences between in vivo participants and donors of the postmortem specimens.

The neuroanatomic cellular underpinnings of the radiologic STh and its disappearance in Parkinson disease must be further investigated. The nonequivalence of STh and nigrosome 1 does not affect the value of STh as a late-stage Parkinson disease biomarker. However, a more accurate link of MRI features and the substantia nigra anatomy is expected to improve Parkinson disease diagnostics and disease monitoring.

Acknowledgments: We thank Patrick Scheibe, PhD, for his help with data visualization and Rawien Balesar, MSc, for sharing his histology expertise. We thank the whole-body donors and acknowledge the whole-body donation program at the University of Maastricht for providing postmortem brain samples.

Author contributions: Guarantors of integrity of entire study, M.B., E.K., N.W.; study concepts/study design or data acquisition or data analysis/interpretation, all authors; manuscript drafting or manuscript revision for important intellectual con-

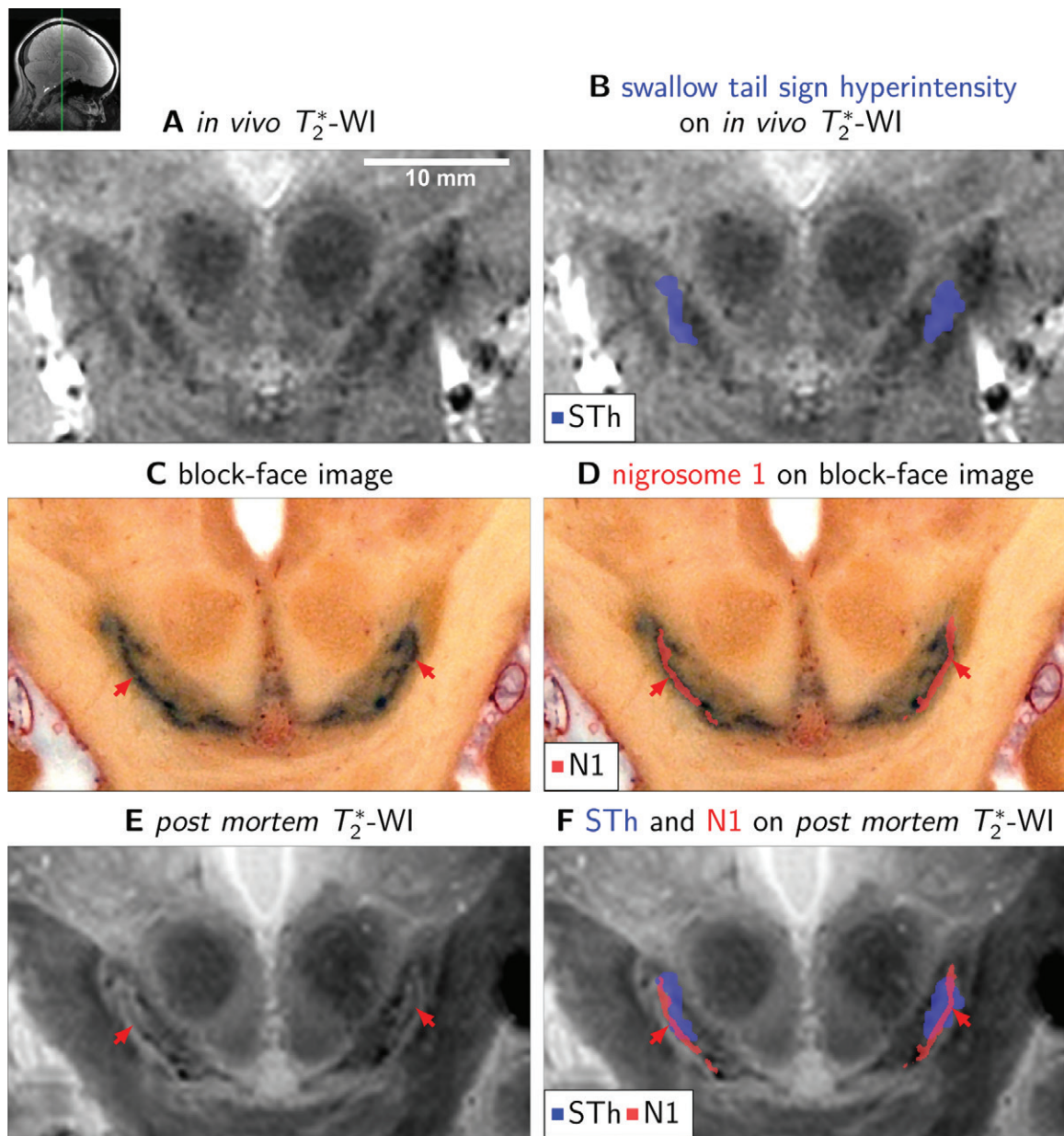


Figure 2: The hyperintense inner part of the swallow tail sign on T2*-weighted images (STh) and nigrosome 1 (N1) overlap partially but show distinct geometry. **(A, B)** In vivo T2*-weighted images (T2*-WI) in a 29-year-old woman. The ovoid STh (Fig 1C) was segmented consistently (mean intrarater Dice coefficient, 0.51 ± 0.14 [SD]). On oblique coronal sections, it had a width of $2.2 \text{ mm} \pm 0.5$ and a length of $5.3 \text{ mm} \pm 1.0$ (mean \pm SD across STh masks and hemispheres). **(C, D)** Oblique coronal postmortem block-face images in a 75-year-old female cadaver show nigrosome 1 (arrows) as an elongated, bent stripe with a width of $0.8 \text{ mm} \pm 0.3$ and a length of $7.1 \text{ mm} \pm 1.1$ (mean \pm SD across hemispheres). Thus, nigrosome 1 was significantly thinner ($P < .001$) and longer ($P = .003$) than the STh. **(E)** On a postmortem T2*-weighted image from same cadaver as in **C** and **D**, nigrosome 1 appears consistently as a hypointense stripe (arrows). **(F)** After coregistration to postmortem T2*-weighted image, nigrosome 1 (arrows) and STh appeared as distinct and only partly overlapping structures. Their mean Dice coefficient was 0.18 ± 0.08 .

tent, all authors; approval of final version of submitted manuscript, all authors; agrees to ensure any questions related to the work are appropriately resolved, all authors; literature research, M.B., E.K., A.A., C. Jantzen, C. Jäger, A.H., P.A.G., M.M., N.W.; clinical studies, A.H.; experimental studies, M.B., E.K., A.A., P.L.B., C. Jantzen, C. Jäger, A.H., K.J.P., P.A.G., M.M., N.W.; statistical analysis, M.B., E.K., A.H.; and manuscript editing, all authors

Disclosures of conflicts of interest: M.B. No relevant relationships. E.K. No relevant relationships. A.A. No relevant relationships. P.L.B. No relevant relationships. C. Jantzen No relevant relationships. C. Jäger No relevant relationships. A.H. No relevant relationships. K.J.P. No relevant relationships. P.A.G. Research contract with ASG; payment or honoraria for lectures, presentations, speak-

ers bureaus, manuscript writing, or educational events from the Institute of Physics Publishing; support for attending meetings and/or travel from ISMRM; secretary of ISMRM. M.M. No relevant relationships. B.U.F. No relevant relationships. N.W. The Max Planck Institute for Human Cognitive and Brain Sciences has an institutional research agreement with Siemens Healthcare; patent on acquisition of MRI data during spoiler gradients (US 10,401,453 B2); speaker at an event organized by Siemens Healthcare and was reimbursed for the travel expenses.

References

- Blazejewska AI, Schwarz ST, Pitiot A, et al. Visualization of nigrosome 1 and its loss in PD: pathoanatomical correlation and in vivo 7 T MRI. *Neurology* 2013;81(6):534–540.

2. Damier P, Hirsch EC, Agid Y, Graybiel AM. The substantia nigra of the human brain. II. Patterns of loss of dopamine-containing neurons in Parkinson's disease. *Brain* 1999;122(Pt 8):1437–1448.
3. Lee H, Baek S-Y, Chun SY, Lee JH, Cho H. Specific visualization of neuromelanin-iron complex and ferric iron in the human post-mortem substantia nigra using MR relaxometry at 7T. *Neuroimage* 2018;172:874–885.
4. Brammerloh M, Morawski M, Friedrich I, et al. Measuring the iron content of dopaminergic neurons in substantia nigra with MRI relaxometry. *Neuroimage* 2021;239:118255.
5. Kirilina E, Helbling S, Morawski M, et al. Superficial white matter imaging: Contrast mechanisms and whole-brain in vivo mapping. *Sci Adv* 2020;6(41):eaaz9281.
6. Alkemade A, Pine K, Kirilina E, et al. 7 Tesla MRI Followed by Histological 3D Reconstructions in Whole-Brain Specimens. *Front Neuroanat* 2020;14:536838.